Supporting Information

Supplementary Information: The Origin of Enhanced Conductivity and Structure Change in Defective $Li_4Ti_5O_{12}$: a study combining theoretical and experimental perspectives

Yu-Te Chan,[a,b‡] Cristina Grosu, [*a,c‡], Matthias Kick[a,b], Peter Jakes[c], Thomas Gigl[d], Stefan Seidlmayer[e], Werner Egger[f], Rüdiger-A. Eichel[c,g], Josef Granwehr[c,h], Christoph Hugenschmidt[d] and Christoph Scheurer[a,b]

[a] *Chair for Theoretical Chemistry and Catalysis Research Center, Technical University of Munich, Lichtenbergstr. 4, 85747 Garching, Germany*

[b] *Fritz-Haber-Institut der Max-Planck-Gesellschaft, 14195 Berlin, Germany*

[c] *Institute of Energy and Technologies (IET-1), Forschungszentrum Jülich, 52425 Jülich, Germany*

[d] *Heinz Maier-Leibnitz Zentrum (MLZ), Technical University of Munich, Lichtenbergstr. 1, 85748 Garching, Germany*

[e] *Heinz Maier-Leibnitz Zentrum (MLZ), Technical University of Munich, Lichtenbergstr. 1, 85748 Garching, Germany*

[f] *Institut für Angewandte Physik und Messtechnik LRT2, Werner-Heisenberg-Weg 39, D-85577 Neubiberg, Germany*

[g] *RWTH Aachen University, Institute of Physical Chemistry, D-52074 Aachen, Germany*

[h] *RWTH Aachen University, Institute of Technical and Macromolecular Chemistry, D-52074 Aachen, Germany*

S1 Experimental details

S1.1 Sample preparation and characterization

S1.1.1 Thermogravimetric analysys with a mass spectrometer (TGA-MS) for the sample preparation

In order to ensure the synthesis of $Li_4Ti_5O_{12}$ LTO with oxygen defects, a thermogravimetric analysys with a mass spectrometer (TGA/MS) instrument, was used to monitor the annealing treatment. All the measurements were performed with a TGA/DSC1 STARe SYSTEM (Mettler Toledo, Switzerland), which is combined with a mass spectrometer (MS) as gas analysis system (Pfeiffer Vacuum, Germany). The synthesis were performed in the temperature range of 25 °C - 700/750 °C using sapphire crucibles (Ø 12 mm) in Ar/H_2 5% atmosphere at a heating rate of 5 K/min. The TGA connected with the MS gas analysis allows us to identify the components released during the heating treatment (in a classic way the decomposition of the investigated samples). Hence, we can confirm the depletion of the oxygen from our pristine LTO. We create a series of defective or the so called"blue" LTO starting from the commercial "white" LTO (Süd Chemie, now Clariant). We prepared the blue LTO by varying the time holding at the annealing temperature 700-750 °C from five minutes to eight hours S1. The intensity of blue theoretically corresponds to a different oxygen concentration.

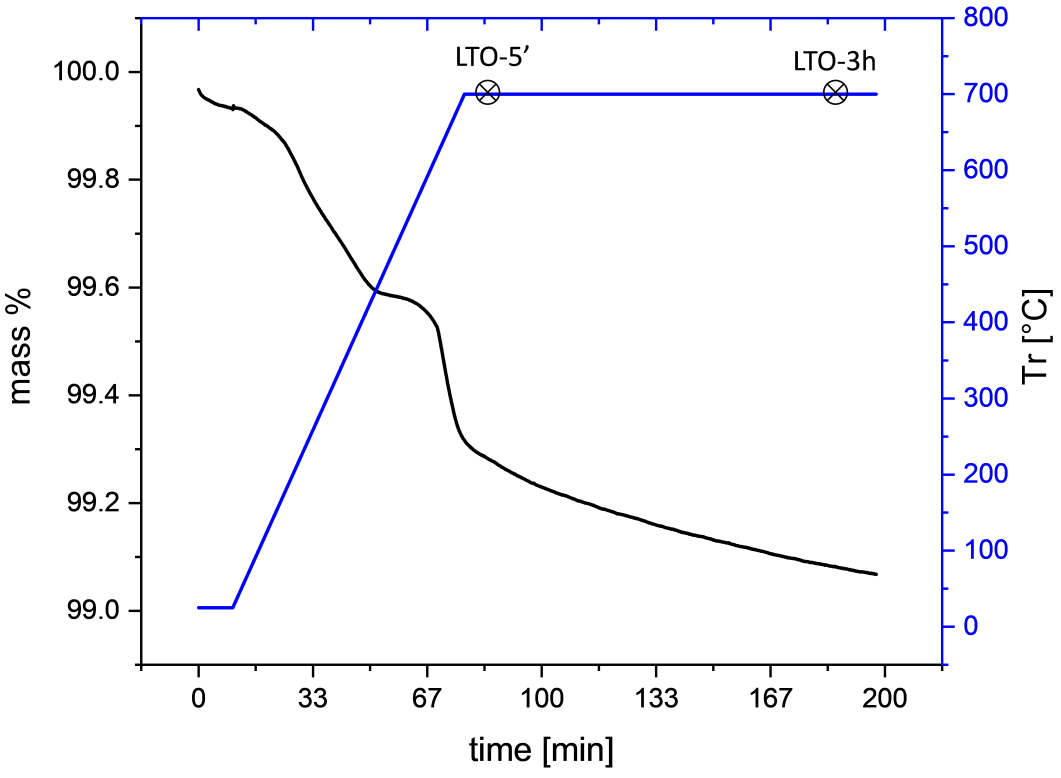

Figure S1: Thermogravimetric analysis for the pristine $Li_4Ti_5O_{12}$. LTO-5' and LTO-3h indicate two examples with the variation of the holding time, once the annealing temperature of 700 °C was reached.

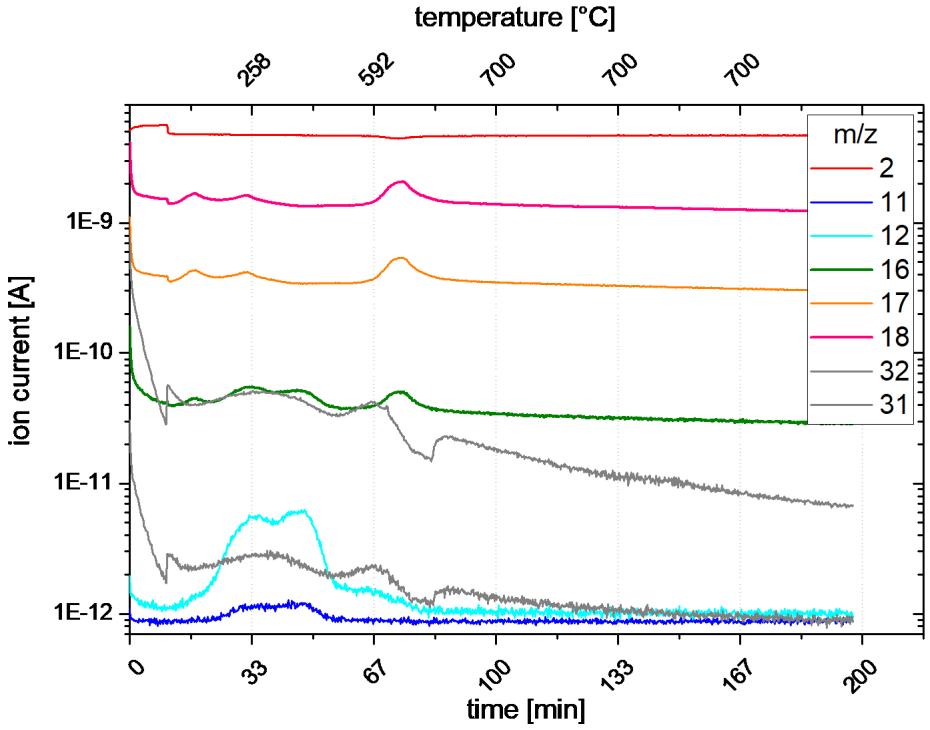

Figure S2: Thermogravimetric analysis and mass spectrometric measurements, while performing the annealing protocol for tailoring the oxygen vacancy formation in $Li_4Ti_5O_{12}$ in an Ar/5 % H_2 atmosphere. The decrease in the signal at m/z 32 (O_2), with the raise in m/z 18 (H_2O) within the temperature range of 592 till 700 °C is an indication of the oxygen depletion from the pristine $Li_4Ti_5O_{12}$.

S1.2 Samples Characterization

S1.2.1 Powder X-ray measurements and the Rietveld refinement strategy

Rietveld Refinement was done with FullProf v7.95 (Jan 2023). All phases were refined with Thomson-Cox-Hastings profile functions convoluted with an asymmetry correction according to the Finger-Cox-Jephcoat approximation as implemented in FullProf. Asymmetry parameters were constrained for all phases. Background was refined with a Chebychev-Polynomial with 10 Parameters.

Initial structure models for refinement:
LTO blue: $Li_4Ti_5O_{12}$ (ICSD-#160655)
TiO_2 rutile-type (ICSD-#121636)
TiO_2 hollandite-type (ICSD-#120242)

Refinement results:
$R_{exp} = 2.74, R_{wp} = 0.0682, Chi^2 = 6.35$
R_{Bragg} LTO blue = 0.021

Phase 1 : LTO blue (mass fraction ≈ 98(1) %)

Composition from refinement : $Li_{1.43(11)}Ti_{1.50}2(45)O_4$ cubic, ($Fd\bar{3}m$) (No. 227), $Z = 8$, a = 8.3644(3) Å

Used restrains: Occ(Ti1) + Occ(Li1) = 1
Refined Profile Parameters: U=0.14(2), W = 0.0012(3), X=0.17(1), D/L = S/L = 0.239(2)

Comment: From compositional refinement the calculation of charge balance reveals a missing charge of −0.562 points to additional oxygen vacancies (≈ 7%), not obtainable from XRD refinement. Additionally,

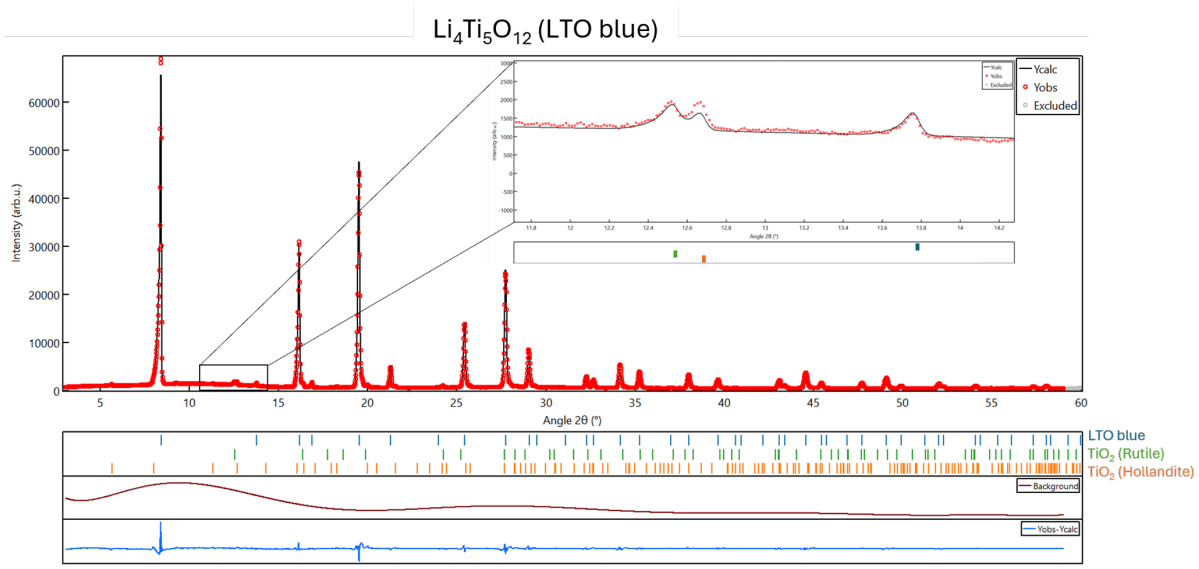

Figure S3: Rietveld refinement of $Li_4Ti_5O_{12}$ (LTO blue) of the X-ray powder diffraction pattern using three phase for refinement. Main phase LTO blue. Impurity phases TiO_2 rutile-type and TiO_2 in an empty hollandite-type.The XRD pattern were recorded with Mo K_{α_1} radiation ($\lambda = 0.70932$ Å, $\tilde{5}0\ keV$, $40\ mA$)

Atom	site	x	y	z	B_{iso}	Occ.
Ti1	16d	1/2	1/2	1/2	0.43(8)	0.75(2)
Li2	16d	1/2	1/2	1/2	0.43(8)	0.25(2)
Li1	8a	1/8	1/8	1/8	1(1)	0.9(1)
O1	32e	0.2620(5)	0.2620(5)	0.2620(5)	0.9(2)	1

Table S1: Parameters from the Rietveld refinement for the blue or defective LTO

the refinement shows Li vacancies ($\approx 10\%$) on 8a.

Phase 2: TiO_2-rutile (mass fraction $\approx 0.90(6)$ %) tetragonal, $P42/mnm$ (No. 136),
a = 4.592(4) Å, c = 2.966(5) Å
Refined Profile Parameters: W = 0.003(10), X=0.4(6), D/L = S/L = 0.239(2)

Phase 3: TiO_2-hollandite (mass fraction $\approx 1.18(6)$ %) tetragonal, $I4/m$ (No. 87),
a = 10.155(6) Å, c = 2.966(3) Å
Refined Profile Parameters: U=0.2(3), Y=0.02(4), D/L = S/L = 0.239(2)

Refinement results:
$R_{exp} = 4.22, R_{wp} = 0.0512, Chi^2 = 1.47$
R_{Bragg} LTO white = 0.0424

Phase 1 : LTO white (mass fraction $\approx 98(2)$ % Composition from refinement : $Li_{1.526(42)}Ti_{1.474(42)}O_4$ cubic, ($Fd\bar{3}m$), (No. 227), Z = 8, a = 8.3654(2) Å

Used restrains: Occ(Ti1) + Occ(Li1) = 1
Refined Profile Parameters: W = 0.0006(1), X=0.292(8), D/L = S/L = 0.211(2)

Comment: From compositional refinement the calculation of charge balance reveals a missing charge of -0.569. This points to additional oxygen vacancies (≈ 7 %), not obtainable from XRD refinement. The Li1 occupation refinement indicates no Li vacancies on the 8a site for LTO white.

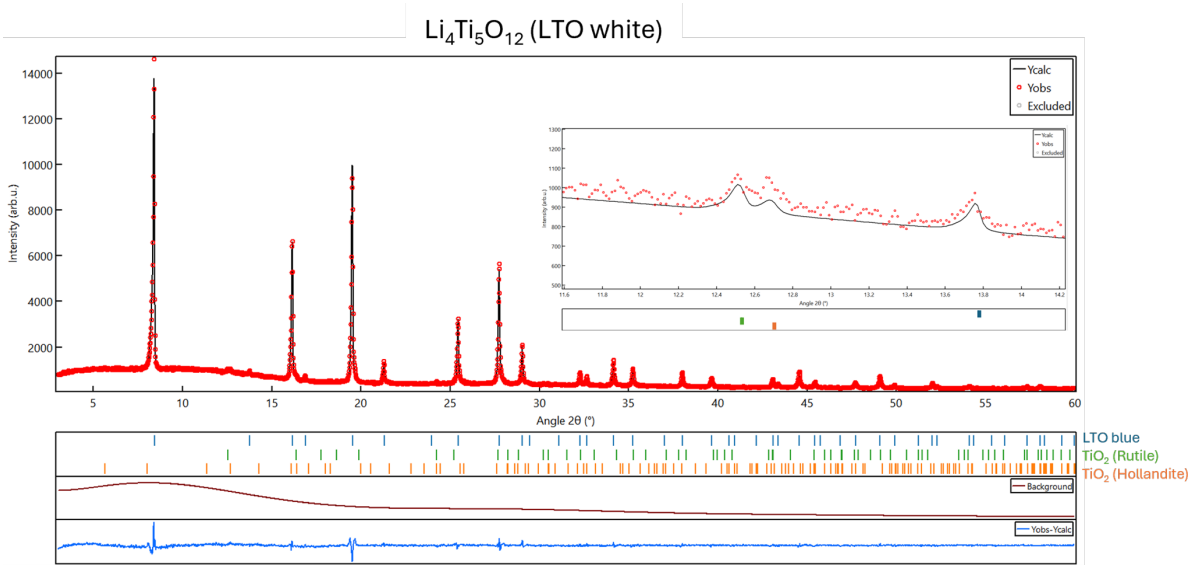

Figure S4: Rietveld refinement of pristine $Li_4Ti_5O_{12}$ (LTO white) of the X-ray powder diffraction pattern using three phase for refinement. Main phase LTO white. Impurity phases TiO_2 rutile-type and TiO_2 in an empty hollandite-type.The XRD pattern were recorded with Mo K_{α_1} radiation ($\lambda = 0.70932$ Å, 50 keV, 40 mA)

Atom	site	x	y	z	B_{iso}	Occ.
Ti1	16d	1/2	1/2	1/2	0.52(7)	0.74(2)
Li2	16d	1/2	1/2	1/2	0.52(7)	0.26(2)
Li1	8a	1/8	1/8	1/8	1.9(10)	1.01(9)
O1	32e	0.2620(5)	0.2620(5)	0.2620(5)	1.0(2)	1

Table S2: Parameters from the Rietveld refinement for the white or pristine LTO

Phase 2 : TiO_2-rutile (mass fraction ≈ 0.8(1) %) tetragonal, $P42/mnm$ (No. 136),
a = 4.595(3) Å, c = 2.964(3) Å
Refined Profile Parameters: W = 0.003(9), X=0.1(4), D/L = S/L = 0.211(2)

Phase 3 : TiO_2-hollandite (mass fraction ≈ 1.2(2)%) tetragonal, $I4/m$ (No. 87),
a = 10.140(7) Å, c = 2.972(4) Å
Refined Profile Parameters: U = 0.3(20), Y=0.05(6), D/L = S/L = 0.211(2)

S1.2.2 Positron Annihilation Lifetime spectroscopy (PALS) and Coincidence Doppler Broadening Spectroscopy (CDBS)

The positron can be assessed accordingly to the beam intensity at different depths within the material from the surface to the bulk. The main difference is located within the 0.5-7 keV range that goes deep into the surface layer till 5 keV and then continues within the bulk material 18-20 keV. Those it is necessary to scan at first over the beam intensity in order to identify the two energies for surface and bulk measurements for LTO. S parameters is the one scanned over the energies, the fact that decreases till 5 keV Figure S6 indicates a higher concentration of the defect on the surface, confirmed later by the more detailed CDBS. We defined those based on Vehanen et al.[1], where we can base the depths on the attenuation of the signal from the positrons based on the different properties of the materials, under the penetration at a certain energy[2]. Here, the following equation 1 was used to identify the average penetration depth.

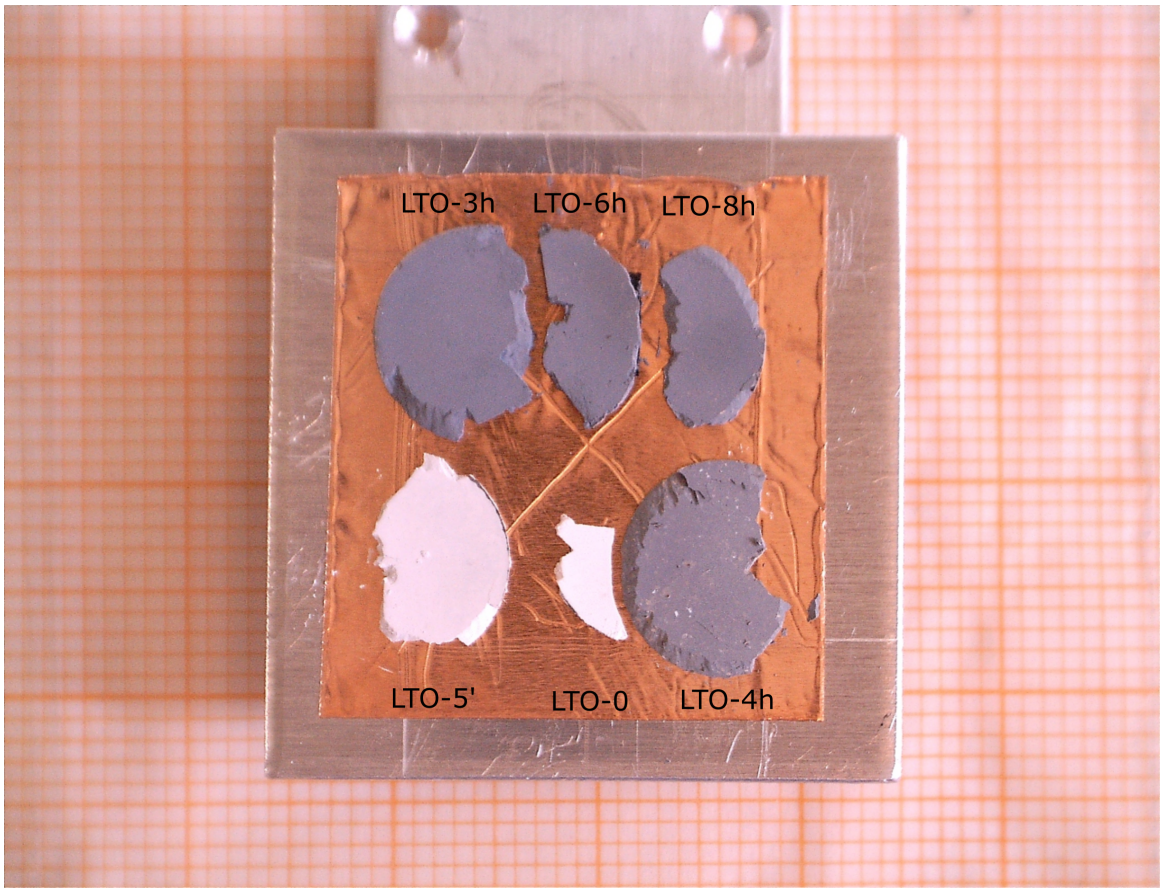

Figure S5: Sample holder for the Coincidence Doppler broadening spectroscopy (CDBS) measurements with the pristine "white" LTO and the "defective" LTO, varying the annealing time.

$$z = 40 \times E^{1.6}/\rho \tag{1}$$

Where z will correspond to the depth in nm, E will be the energy, and ρ the density of the material. The numbers are constants.

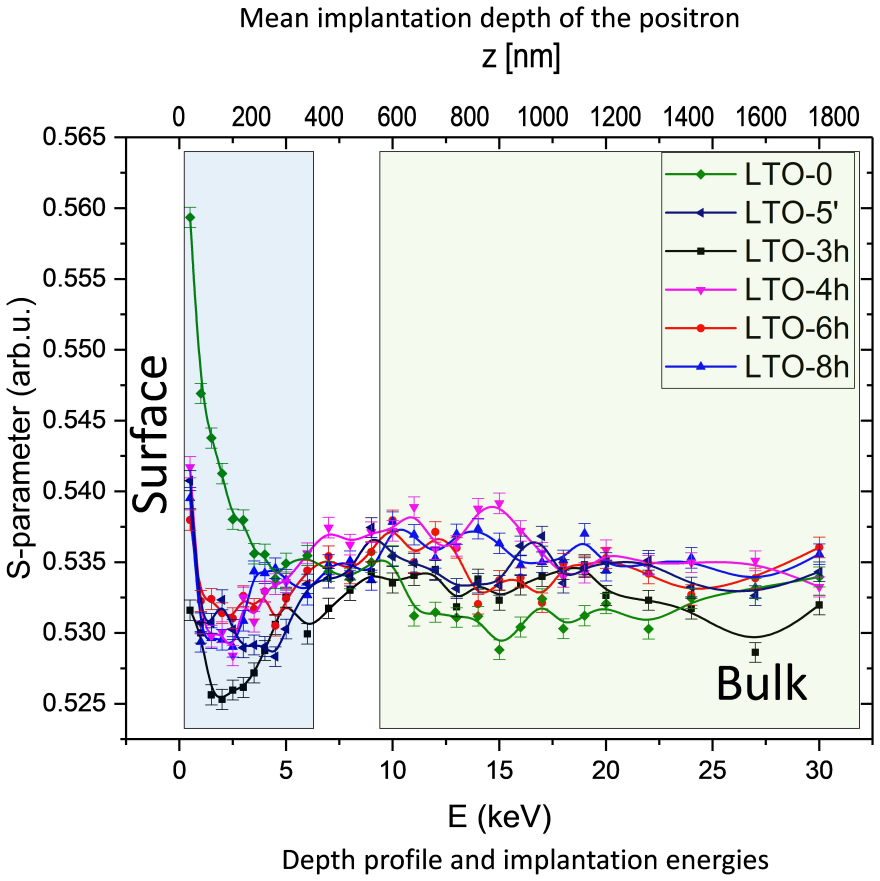

Figure S6: S-parameters scans as function of incident positron energy. Energies within the range of 1-5 keV correspond to surface regions. Energies higher than 18 keV identifies the bulk region/defects.

S2 Theoretical details

S2.1 LTO bulk

LTO bulk configurations with Li^{16d} disorder were initially screened using force fields[3]. Distinct series ('bulk 1', 'bulk 2', and 'bulk 3') with varying Li^{16d} configurations were evaluated with DFT calculations. Their DFT-calculated relative energies and bandgaps are presented in Figure S7. The most energetically stable configuration from each of these three series was selected, yielding the final Bulk 1, Bulk 2, and Bulk 3 models. These three models were specifically constructed with their z-axes oriented along the (111), (110), and (100) crystallographic directions, respectively, for the subsequent creation of surface slabs. Figure S8 shows their distinct Li^{16d}-Li^{16d} radial distribution functions (RDFs), confirming unique Li^{16d} ordering in each. This sampling strategy thus provided diverse and computationally tractable LTO models, pre-oriented for comprehensive surface investigations.

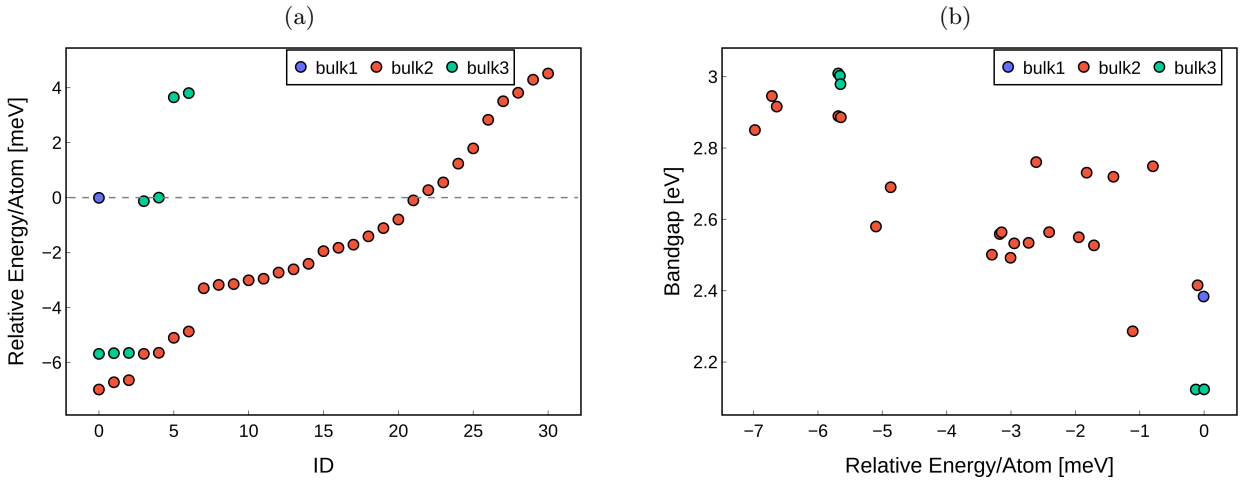

Figure S7: (a) DFT relative energies and (b) bandgaps for candidates pre-screened by force fields.

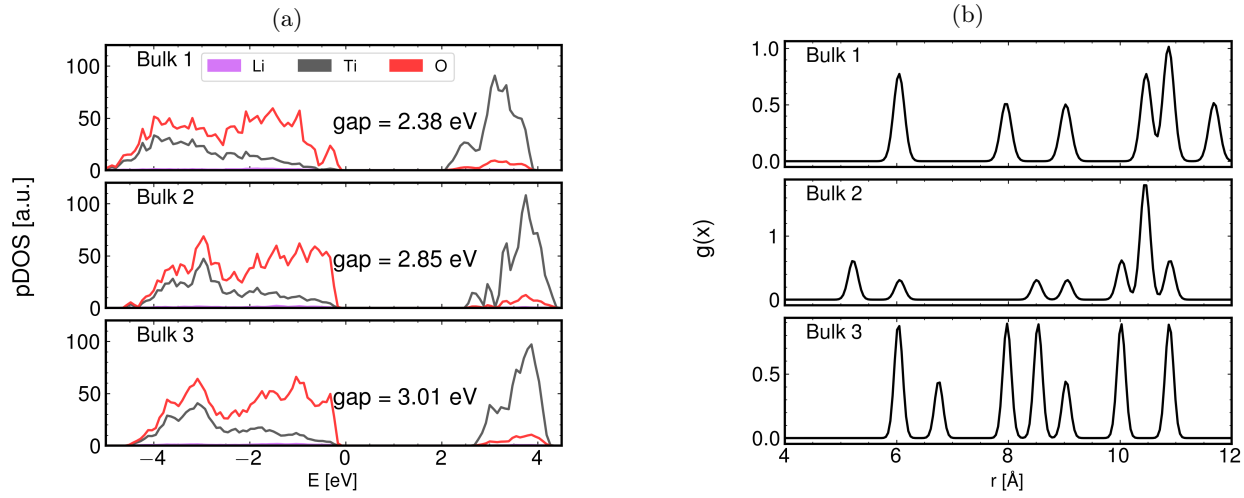

Figure S8: (a) Projected Density of States (PDOS). (b) The Li^{16d}-Li^{16d} RDFs

S2.2 Positron-electron interaction benchmark

There is no study on LTO positron lifetime both from theoretical and experimental sides. On the other hand, TiO_2 has experimental measurement on positron lifetimes from more than one studies. Zheng et al. studied the positron lifetime change along the Ruile-Anatase phase transition via temperature control[4]. Based on their findings, Anatase$-TiO_2$ will become Rutile$-TiO_2$ completely when temperature reach 750 °C. The positron lifetime measured on the sample change from 201 ± 5 ps to 134 ± 3 ps. Valeeva et al. reported a similar positron lifetime, 148 ± 4 ps, for Rutile$-TiO_2$[5]. Arguably, the same methods which can describe TiO_2 positron lifetimes well should be able to describe LTO since the two out of three elements in LTO are identical (even the oxidation states) with TiO_2, except Li. Moreover, most of the positron density should distribute around oxygen, which attract positron more. In Table S3, we compare the positron lifetime from different methods on dealing with positron-electron interactions. More details of the electron-positron correlation functional and enhancement factor used in each method can be found on abinit website[6]. In general, we found that LDA (ixcpositron = 1, 2, 11) gives lifetimes more close to the experimental values for TiO_2. However, it's hard to describe localized positrons in model with voids, i.e. surface and vacancy models. In fact, based on our experience, LDA can not convergence well for localized systems. Thus, in the present work, LDA(ixcpositron = 11) is used for systems with delocalized positron (i.e. bulk), and GGA (ixcpositron = 3) is used for localized systems.

Table S3: Positron lifetime from different methods.

	exp.	ixcpositron				
		1	2	11	3	31
Rutile$-TiO_2$[7]	134 ± 3 ps[4]	154.71 ps	154.62 ps	156.50 ps	177.38 ps	179.22 ps
	148 ± 4 ps[5]					
Anatase$-TiO_2$[7]	201 ± 5 ps[4]	189.69 ps	190.28 ps	191.11 ps	222.33 ps	223.86 ps
BBC$-$Li	291 ± 6 ps	306.08 ps	310.49 ps	303.43 ps	321.20 ps	317.86 ps
LTO$-$bulk[8]		185.86 ps	186.47 ps	187.13 ps	219.70 ps	220.87 ps

The k-grids generated by the Monkhorst-Pack scheme used for Rutile$-TiO_2$, Anatase$-TiO_2$, BCC$-$Li and LTO-bulk are [4, 4, 6], [5, 5, 2], [5, 5, 5], and [4, 4, 2] respectively. More details can be found in Table S4

Table S4: Model information

Model Name	Number of Atoms	Cell Parameters (Å)	K-Grids
LTO Bulk 1	42	(5.973, 0.000, 0.000) (-2.980, 5.161, 0.000) (0.000, 0.000, 14.610)	4 x 4 x 2
LTO Bulk 2	84	(6.028, 0.002, 0.006) (0.007, 18.131, -0.021) (0.009, -0.010, 8.535)	4 x 2 x 4
LTO Bulk 3	84	(6.035, 0.000, 0.000) (0.000, 6.032, -0.016) (0.000, -0.068, 25.591)	4 x 4 x 2
LTO V_{Li}	167	(12.115, -0.007, 0.000) (-6.051, 10.479, 0.020) (0.000, 0.028, 14.766)	2 x 2 x 2
LTO V_O	167	(12.167, -0.007, -0.000) (-6.076, 10.471, 0.014) (-0.000, 0.020, 14.720)	2 x 2 x 2
LTO (111) surface	168	(11.946, 0.000, 0.000) (-5.960, 10.323, 0.000) (0.000, 0.000, 29.221)	2 x 2 x 1
LTO (110) surface	168	(8.498, 0.000, 0.000) (0.000, 12.159, 0.000) (0.001, 0.001, 33.536)	4 x 2 x 1
LTO (100) surface	168	(11.972, 0.007, 0.134) (0.004, 6.039, 0.002) (0.460, 0.015, 41.153)	2 x 4 x 1
Rutile−TiO_2	6	(4.594, 0.000, 0.000) (0.000, 4.594, 0.000) (0.000, 0.000, 2.959)	4 x 4 x 6
Lithiated Rutile−TiO_2 ($LiTiO_2$)	8	(5.035, 0.000, 0.000) (0.000, 5.035, 0.000) (0.000, 0.000, 3.213)	4 x 4 x 6
Anatase−TiO_2	12	(3.784, 0.000, 0.000) (0.000, 3.784, 0.000) (0.000, 0.000, 9.514)	5 x 5 x 2
Lithiated Anatase−TiO_2 ($LiTiO_2$)	8	(5.131, 0.000, 0.000) (1.872, 4.778, 0.000) (-3.502, -2.389, 2.892)	2 x 2 x 4
BCC−Li	2	(3.509, 0.000, 0.000) (0.000, 3.509, 0.000) (0.000, 0.000, 3.509)	5 x 5 x 5

S2.3 Lithiated TiO_2

The 83 ps lifetime component observed in our samples, potentially linked to Li-ion dynamics within TiO_2 impurity domains. TiO_2, whether as rutile or anatase, is well-documented to undergo electrochemical lithiation[9,10]. This process induces significant structural transformations and volumetric changes, which are highly dependent on the polymorph, lithium content, and material dimensionality. For instance, in situ studies on rutile TiO_2 nanostructures reveal a two-step transformation: first to an irreversible monoclinic phase at partial lithiation (Li_xTiO_2 with x∼0.5), and subsequently to a rock-salt phase upon near-full lithiation ($LiTiO_2$). These transformations are accompanied by large, anisotropic volumetric expansion (total volumetric expansion of the nanowire is approximately 120%) and distortion[9]. Nanoscale anatase TiO_2 can achieve full $LiTiO_2$ stoichiometry, particularly in crystallites smaller than 10 nm where the phase transformation is complete, forming a phase with altered lattice parameters that differs from bulk behavior; this $LiTiO_2$ phase may preferentially form at particle surfaces in larger nanoparticles. Such structural modifications would inherently induce substantial strain if the TiO_2 domains are confined within a host matrix like LTO. The insertion of Li leads to the reduction of Ti^{4+} to Ti^{3+} (electron polarons), which could be one of the origins of volume expansion observed experimentally[10]. Given the documented phase complexity and the strong influence of particle size and lithium concentration on the resulting structures and properties of lithiated TiO_2, our simplified modeling approach aims to explore the behavior of such confined impurity phases and their potential contribution to the observed positron annihilation lifetime characteristics. Accordingly, we modeled two series representing fully lithiated TiO_2 (both rutile and anatase polymorphs). These were subjected to mild volumetric compression to simulate the confinement effects anticipated from the LTO framework. The TCDFT computed positron lifetimes for these series, presented as a function of relative volume change, are shown in Figure S9. As depicted in Figure S9, the positron lifetime for the lithiated rutile TiO_2 series is lower (by approximately 15 ps at comparable material volumes) than that of pristine rutile TiO_2. This lifetime decreases further with increasing compressive strain. For the fully lithiated anatase TiO_2 series, the computed lifetimes range from approximately 131 ps down to 95 ps as compressive strain increases.

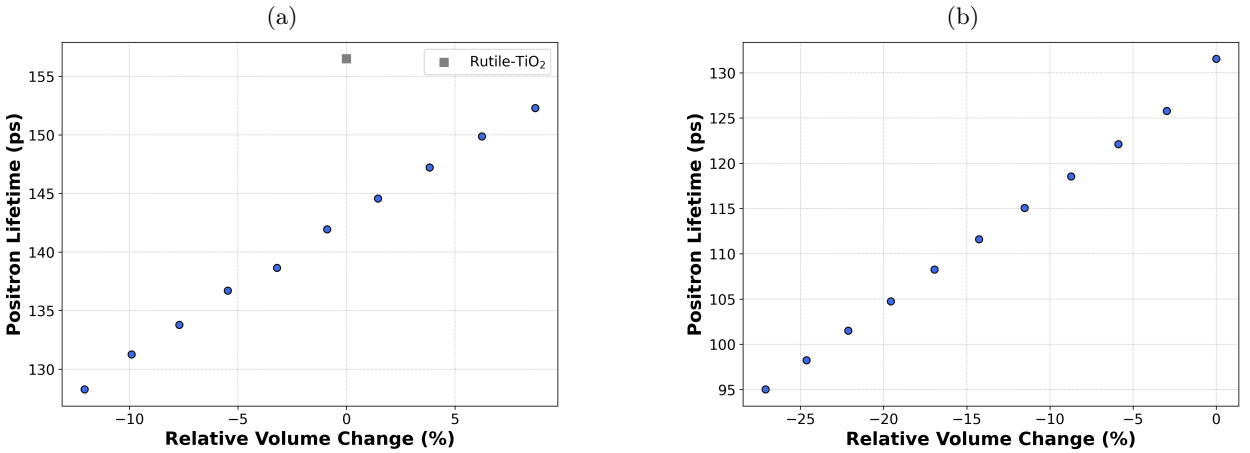

Figure S9: TCDFT computed positron lifetimes for (a) fully lithiated rutile ($LiTiO_2$) and (b) fully lithiated anatase ($LiTiO_2$) series, subjected to mild volumetric compression. Lifetimes are shown as a function of relative volume change. For series (a), the volume change is relative to the uncompressed rutile structure. For series (b), the volume change is relative to the uncompressed fully lithiated anatase structure (referenced from Materials Project, mp-38280). The grey dot indicates the computed lifetime for pristine rutile TiO_2 for comparison.

Reference

[1] A. Vehanen, K. Saarinen, P. Hautojärvi and H. Huomo, *Phys. Rev. B Condens. Matter*, 1987, **35**, 4606–4610.

[2] R. Brusa, S. Mariazzi, L. Ravelli, P. Mazzoldi, G. Mattei, W. Egger, C. Hugenschmidt, B. Löwe, P. Pikart, C. Macchi and A. Somoza, *Nuclear Instruments and Methods in Physics Research Section B: Beam Interactions with Materials and Atoms*, 2010, **268**, 3186–3190.

[3] S. Kerisit, K. M. Rosso, Z. Yang and J. Liu, *The Journal of Physical Chemistry C*, 2009, **113**, 20998–21007.

[4] F. Zheng, Y. Liu, Z. Liu, Y.-Q. Dai, P.-F. Fang and S.-J. Wang, *Journal of Crystal Growth*, 2012, **353**, 55–58.

[5] A. A. Valeeva, A. A. Rempel, W. Sprengel and H.-E. Schaefer, *Phys. Chem. Chem. Phys.*, 2003, **5**, 2304–2307.

[6] *Abinit variables*, `https://docs.abinit.org/variables`, 2023, Accessed: Nov 4, 2023.

[7] C. J. Howard, T. M. Sabine and F. Dickson, *Acta Crystallographica Section B*, 1991, **47**, 462–468.

[8] R. W. G. Wyckoff, 1963, **1**, 7–83.

[9] S. J. Kim, S.-Y. Noh, A. Kargar, D. Wang, G. W. Graham and X. Pan, *Chemical Communications*, 2014, **50**, 9932.

[10] W. J. H. Borghols, D. Lützenkirchen-Hecht, U. Haake, E. R. H. van Eck, F. M. Mulder and M. Wagemaker, *Phys. Chem. Chem. Phys.*, 2009, **11**, 5742–5748.